

Multiobjective Nonlinear Model Predictive Control of the Microbial Process

Lakshmi N Sridhar*

Chemical Engineering Department University of Puerto Rico Mayaguez.

*Corresponding Author

Lakshmi N Sridhar, Chemical Engineering Department University of Puerto Rico Mayaguez.

Submitted: 2023, Apr 15; Accepted: 2023, Apr 24; Published: 2023, May 23

Citation: Sridhar, L. N. (2023). Multiobjective nonlinear model predictive control of the microbial process. *Archives Clin Med Microbiol*, 2(2), 27-50.

Abstract

A rigorous multiobjective nonlinear model predictive control is performed on the microbiome dynamic model that takes into account competition, amensalism, parasitism, neutralism, commensalism and cooperation. The optimization language pyomo is used in conjunction with the state of the art global optimization solver BARON. It is demonstrated that when the species that produces the required product is favorable to the other species there is an initial decrease in the required product before an increase happens.

1. Introduction

There has been a lot of research that describe the complex interactions of the many microbial organisms that exist in the microbial cluster in chemostats. The microbial consortium is a complex system with higher-order dynamic characteristics that are governed by commensalism, amensalism, co-operation, neutral behavior and parasitism. To explain these complex interactions, highly sophisticated nonlinear models have been developed. Such nonlinearities pose challenges to the performance of optimization and control tasks. In this article multiobjective nonlinear model predictive control for a dynamic microbiome model is performed using the modeling language Pyomo in conjunction with the state of the art global optimization solver BARON. The document is organized as follows. The background is followed by the description of the model equations and the nonlinear model predictive control strategy. This is followed by the discussion of the results and conclusions

2. Background

Fredrickson & Stephanopoulos and Du et al, discuss the communications between the microbes via metabolic or genetic signals and these interactions are responsible for the resilience of the whole microbial community to adverse conditions [1,2]. Such sustainable resilience may be impossible for the individual cells [3,4]. The advantages that cocultures demonstrate over monocultures include robustness to perturbations, compartmentalization of incompatible reactions and division of labor [5,6]. Microbial coculture or consortia have been applied to configure different sections of metabolic pathways to improve catalytic performance and has led to the production of biofuels and nutritional products [7-11]. Synthetic biology tools such as cell signalling translators and biosensors have been developed to regulate the composition of cultures [12-16]. Microbial interactions are important to develop advanced biomaterials, biofilm formation and

disarm antibiotic resistant superbugs [17-19]. Some researchers, present kinetic models that describe the effect of nutrient and environmental conditions on cell growth [20-22]. Several workers have modified the original Monod model to incorporate extra terms [23-26]. Tsuchiya et al., have formulated a set of coupled Monod equations that exhibit oscillatory behavior [27]. Self-inhibitory factors and nutrient limiting conditions have been incorporated in a hybrid Monod model 10 that accurately describes cell growth.

The Lotka Volterra model describes the dynamic species interaction in closed systems [28,29]. The complex dynamics of the interacting species in the microbial consortia poses challenges to track the population changes in the interacting species. The complexity of the dynamics is because of the presence of singularities such as limit points and branch points (that give rise to multiple trajectories) and Hopf bifurcation points that cause oscillations. The presence of microbes everywhere, and their role in human health has resulted in the design of bacterio-therapies where bacteria is administered to patients for therapeutic purposes. One must clearly understand the details of the microbial dynamics in a colony to be able to the design of resulting therapeutics. The human microbiome constitutes all the microorganisms that live in and on the surface of our bodies. The microbiome plays a significant role in several human diseases [30-35]. Given the microbiome's role in human health, and in the design and development of bacterio-therapies, which are cocktails of several bacteria working together to achieve specific therapeutic effects, it is important to understand the population dynamics in the microbiome.

Stein et al, model microbial dynamics using the continuous time deterministic generalized Lotka-Volterra (gLV) equations, reduce it to a discrete time linear model via a log transform, and use

a L2 penalized linear regression to infer model parameters [36]. Some researchers discuss the ecological interaction types (mutualism, commensalism, amensalism, neutral behavior, competition and exploitation) [37-40]. This led to the development and parameterization of community dynamic models [41-45]. The aim of this paper is to perform rigorous multiobjective nonlinear model predictive control on the microbiome using the model de-

scribed in Xu that takes into account competition, amensalism, parasitism, neutralism, commensalism and cooperation [10]. Details of this model are presented in the next section.

3. Microbiome Model

The equations that govern the microbiome model are [10]

$$\frac{dx_A}{dt} = (\mu_A - D_A)x_A \quad (1)$$

$$\frac{dx_B}{dt} = (\mu_B - D_B)x_B \quad (2)$$

$$\frac{dS}{dt} = D(S_0 - S(t)) - \frac{\mu_A x_A(t)}{Y_{AS}} - \frac{\mu_B x_B(t)}{Y_{BS}} - \frac{(\alpha\mu_A + \beta)x_A(t)}{Y_{PS}} \quad (3)$$

$$\frac{dP_A}{dt} = (\alpha\mu_A + \beta)x_A(t) - DP_A(t) - \frac{kx_B(t)P_A(t)}{Y_{BA}(k_m + P_A(t))} \quad (4)$$

$$\frac{dP_B}{dt} = -DP_B(t) + \frac{kx_B(t)P_A(t)}{(k_m + P_A(t))} \quad (5)$$

$$\mu_A = \frac{\mu_{A_max} S}{K_{SA} + S} \left(1 + \frac{\gamma_{BA} x_B}{S_0 Y_{BS}}\right) \quad (6)$$

$$\mu_B = \frac{\mu_{B_max} S}{K_{SB} + S} \left(1 + \frac{\gamma_{AB} x_A}{S_0 Y_{AS}}\right) \quad (7)$$

The nomenclature in these equations are given by

- μ_{A_max} maximal specific growth rate for species A (1/h)
- μ_A specific growth rate for species A (1/h)
- μ_{B_max} maximal specific growth rate for species B (1/h)
- μ_B specific growth rate for species B (1/h)
- K_{SA} substrate saturation constant for species A (g/L)
- K_{SB} substrate saturation constant for species B (g/L)
- Y_{AS} species A biomass yield from substrate S (g/g)
- Y_{BS} species B biomass yield from substrate S (g/g)
- Y_{BA} product B (PB) yield from intermediate A (PA) (g/g)
- Y_{PS} intermediate A (PA) yield from substrate S (g/g)
- α growth-associated intermediate A (PA) formation coefficient (dimensionless)
- β growth-unassociated intermediate A (PA) formation rate (1/h)
- γ_{AB} interaction coefficient of species A imposes on species B (dimensionless)
- γ_{BA} interaction coefficient of species B imposes on species A (dimensionless)
- k rate constant of intermediate A (PA) converted to product B (PB) (1/h)
- K_m intermediate A saturation constant for species B (g/L)
- x_A species A biomass in the CSTR (g/L)
- x_B species B biomass in the CSTR (g/L)
- P_A intermediate A concentration in the CSTR (g/L)

- P_B product B concentration in the CSTR (g/L)
- S substrate concentration in the CSTR (g/L)
- S_0 substrate concentration in the feeding stream (g/L)
- D dilution rate in the CSTR (1/h)

Chart 1 shows the nature of the interactions when the values of γ_{AB}, γ_{BA} are -1, 0 or 1. These interactions are competition, amensalism, parasitism, neutralism, commensalism and cooperation. The interaction coefficient was defined by a dimensionless factor (γ_{AB}, γ_{BA}) that describe the interactions between species A and B. A pointed arrow indicates beneficial relation, a blunt-ended arrow indicates harmful relation. The other parameter values are $\mu_{A_max} = 1.6/h$; $\mu_{B_max} = 1.2/h$; $K_{SA} = 1.0$ g/L; $K_{SB} = 0.8$ g/L; $S_0 = 50$ g/L; $Y_{AS} = 0.5$ g/g; $Y_{BS} = 0.8$ g/g; $Y_{BA} = 0.8$ g/g; $Y_{PS} = 0.4$ g/g; $\alpha = 0.5$ and $\beta = 0.5$

A \longrightarrow B Commensalism $\gamma_{AB} = 1, \gamma_{BA} = 0$

A \longleftarrow B Amensalism $\gamma_{AB} = -1, \gamma_{BA} = 0$

A \longleftarrow B Commensalism $\gamma_{AB} = 0, \gamma_{BA} = 1$

A \longleftarrow B Amensalism $\gamma_{AB} = 0, \gamma_{BA} = -1$

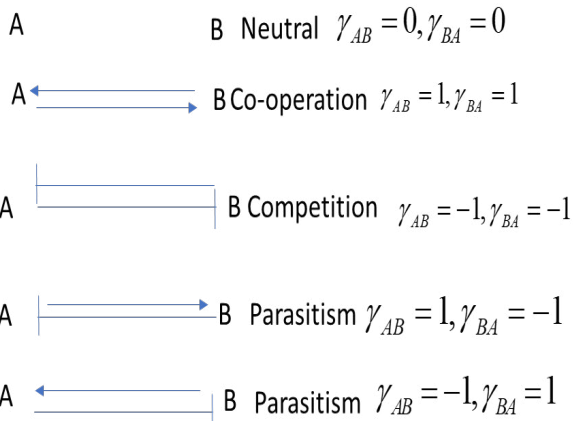


Chart. 1

4. Multiobjective Nonlinear Model Predictive Control (MNL MPC) method

The multiobjective nonlinear model predictive control (MNL MPC) method is used to perform the calculations [46,47]. This method is rigorous and it does not involve the use of weighting functions not does it impose additional parameters or additional constraints on the problem unlike the weighted function or the epsilon correction method For a problem that is posed as

$$\begin{aligned}
 \min J(x, u) &= (x_1, x_2 \dots x_k) \\
 \text{subject to } \frac{dx}{dt} &= F(x, u) \\
 h(x, u) &\leq 0 \\
 x^L &\leq x \leq x^U \\
 u^L &\leq u \leq u^U
 \end{aligned} \tag{8}$$

The MNL MPC method first solves dynamic optimization problems independently minimizing/maximizing each x_i individually [48]. The minimization/maximization of x_i will lead to the values x_i^* . Then the optimization problem that will be solved is

$$\begin{aligned}
 \min \sqrt{\{x_i - x_i^*\}^2} \\
 \text{subject to } \frac{dx}{dt} &= F(x, u) \\
 h(x, u) &\leq 0 \\
 x^L &\leq x \leq x^U \\
 u^L &\leq u \leq u^U
 \end{aligned} \tag{9}$$

This will provide the control values for various times. The first obtained control value is implemented and the remaining discarded. This procedure is repeated until the implemented and the first obtained control value are the same. This will also enable in the drawing of the Pareto Curves which show the variation of the optimal values of one variable with another.

The optimization package in Python, PYOMO where the differential equations are automatically converted to a Nonlinear

Program (NLP) using the orthogonal collocation method The Lagrange-Radau quadrature with three collocation points is used and 10 finite elements are normally chosen to solve the optimal control problems [49]. The resulting nonlinear optimization problem will be solved using the solver Baron BARON implements a Branch-and-reduce strategy to provide valid lower and upper bounds for the optimal solution and provides a guaranteed global optimal solution [50]. This algorithm combines constraint propagation, interval analysis, and the duality in it reduces arsenal with enhanced branch and bound concepts as it winds its way through the hills and valleys of complex optimization problems in search of global solutions. BARON is accessed through the PYOMO-GAMS27.2 interface [51]. To summarize the steps of the algorithm are as follows

1. Minimize/maximize x_i subject to the differential and algebraic equations that govern the process using PYOMO and BARON. This will lead to the value x_i^*
2. Minimize $\sqrt{\{x_i - x_i^*\}^2}$ subject to the differential and algebraic equations that govern the process using PYOMO and BARON. This will provide the control values for various times.
3. Implement the first obtained control values and discard the remaining.
4. Repeat steps 1 to 4 until there is insignificant difference between the implemented and the first obtained value of the control variables.

P_B is the required product that is produced from P_A Hence both P_A and P_B are maximized. The maximization of P_A and P_B will yield the values P_A^* and P_B^* . The function $\sqrt{(P_A - P_A^*)^2 + (P_B - P_B^*)^2}$ is minimized. All the optimization is performed subject to equations 1-7. This is done for various combinations of γ_{AB} and γ_{BA} which individually take on values of -1, 0 and 1. The combinations of γ_{AB} and γ_{BA} are [(0,0), (0,-1), (0,1), (1,0), (1,-1), (1,1), [(-1,0), (-1,-1), (-1,1)]. The dilution rate D is the control variable.

5. Results and Discussion

Figures 1(a, b), 2(a,b),...9(a,b) show the plots of P_A and P_B versus t. Figures 1c-9c show the Pareto surfaces (P_A versus P_B versus t). In all the cases where γ_{BA} is 1 (figures 2a,2b,2c, 5a,5b,5c, 8a,8b,8c) there is an initial monotonic decrease in P_A while P_B first decreases before increasing. In all other cases, there is a monotonic increase in P_A and a monotonic decrease in P_A To understand the cause for this one has to compare P_A the versus t curves for the cases when γ_{BA} is not equal to 1, with the same curve when γ_{BA} is unity. While all the curves show an initial decrease in P_A (in figs 2a and 8a, where γ_{BA} is 1, P_A also increases after an initial decrease) the initial decrease in the cases when γ_{BA} is not equal to 1, is less pronounced than when γ_{BA} is unity. The reason for this is the that initially the conversion of x_A is used in the production of production of x_B and much of the x_B results in more x_A and not in P_A or P_B Hence, $\frac{dP_B}{dt} < 0$ until the value of x_B goes high enough to cause to value of the derivative $\frac{dP_B}{dt}$ to become positive. Therefore, when the interactive coefficient of the species that produces the required product is 1 (or when the species that produces the required product is favorable to the other species) one must wait for sometime before the required product concentration starts to increase.

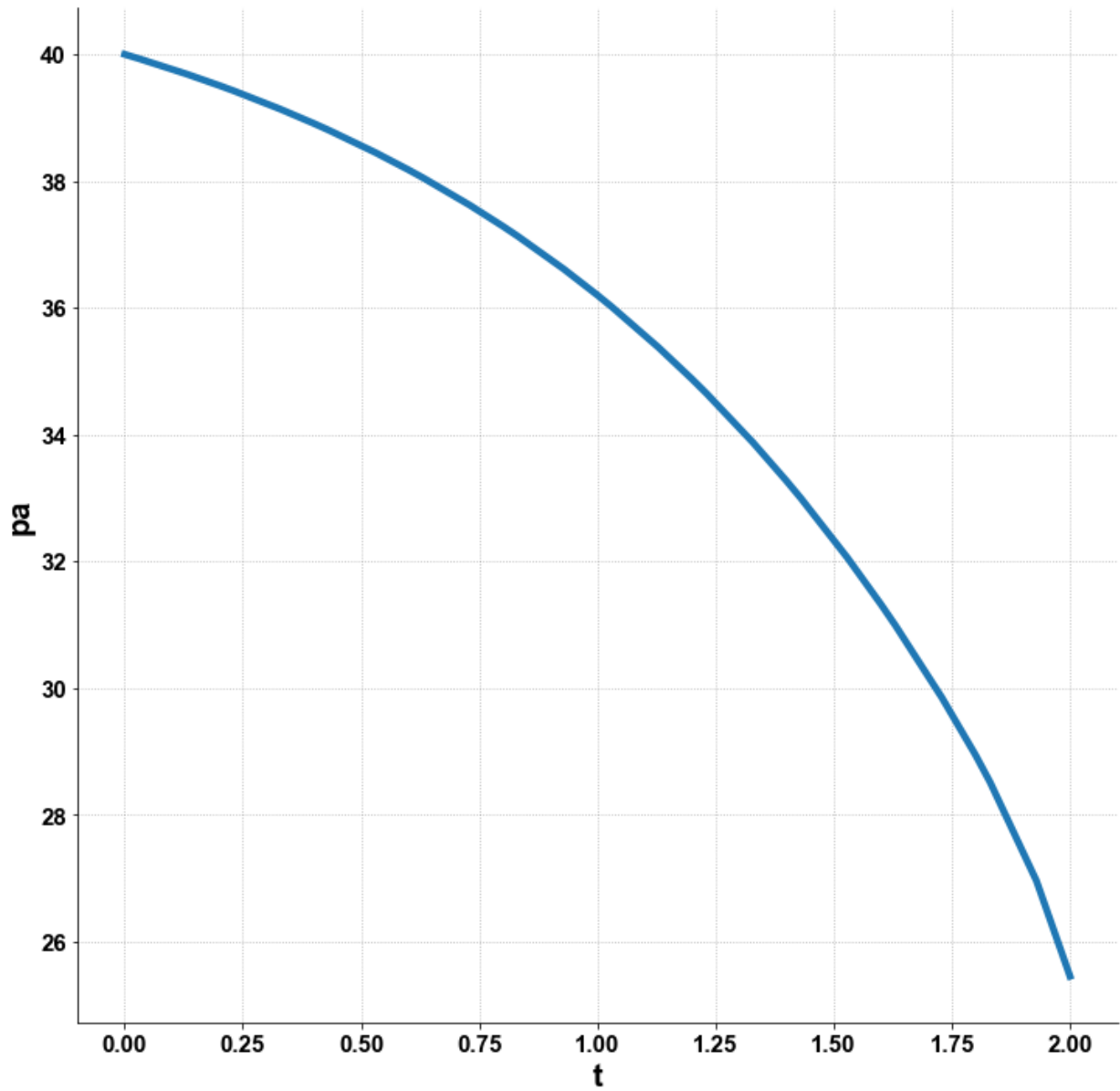


Fig 1a($\gamma_{AB} = 0 ; \gamma_{BA} = 0$)

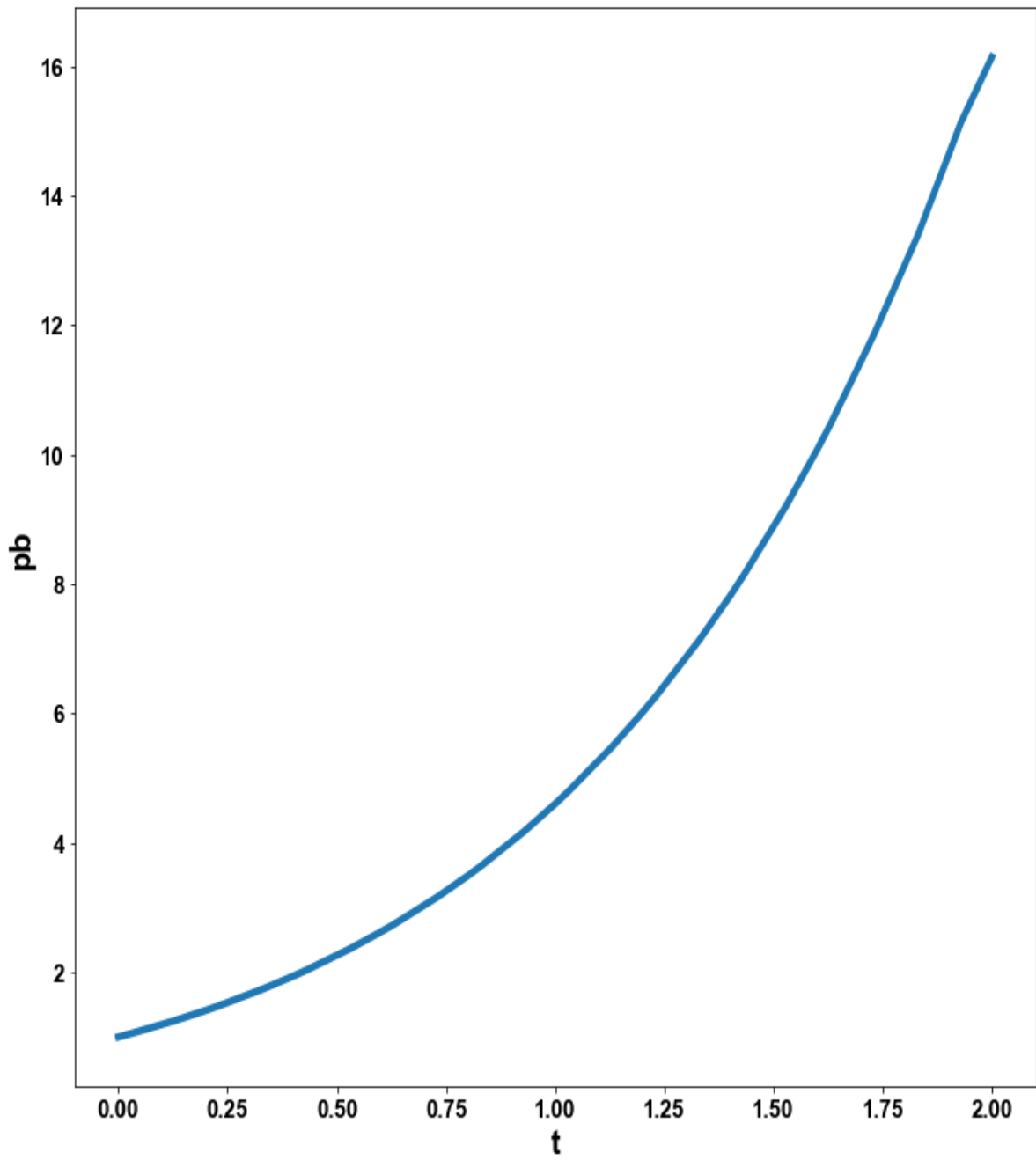


Fig. 1b ($\gamma_{AB} = 0 ; \gamma_{BA} = 0$)

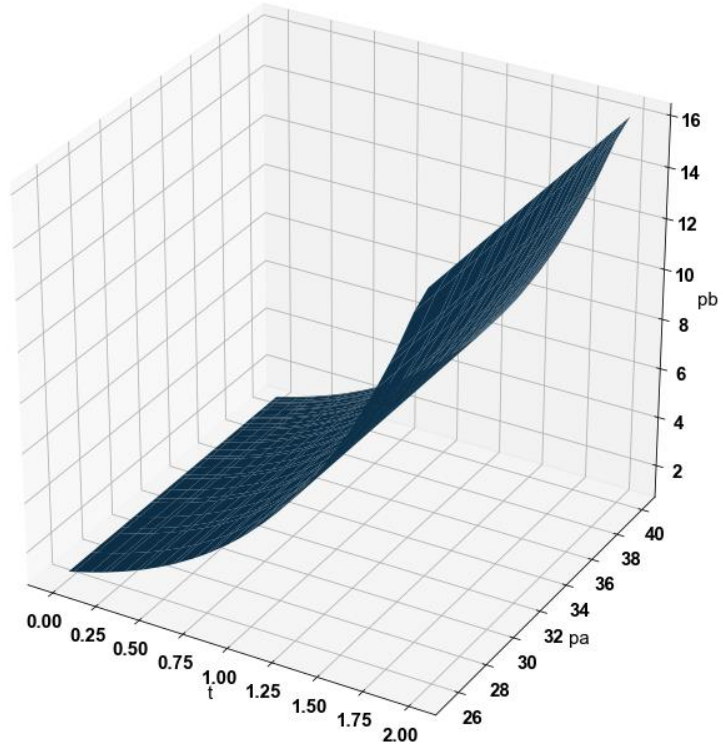


Fig. 1 c ($\gamma_{AB} = 0$; $\gamma_{BA} = 0$)

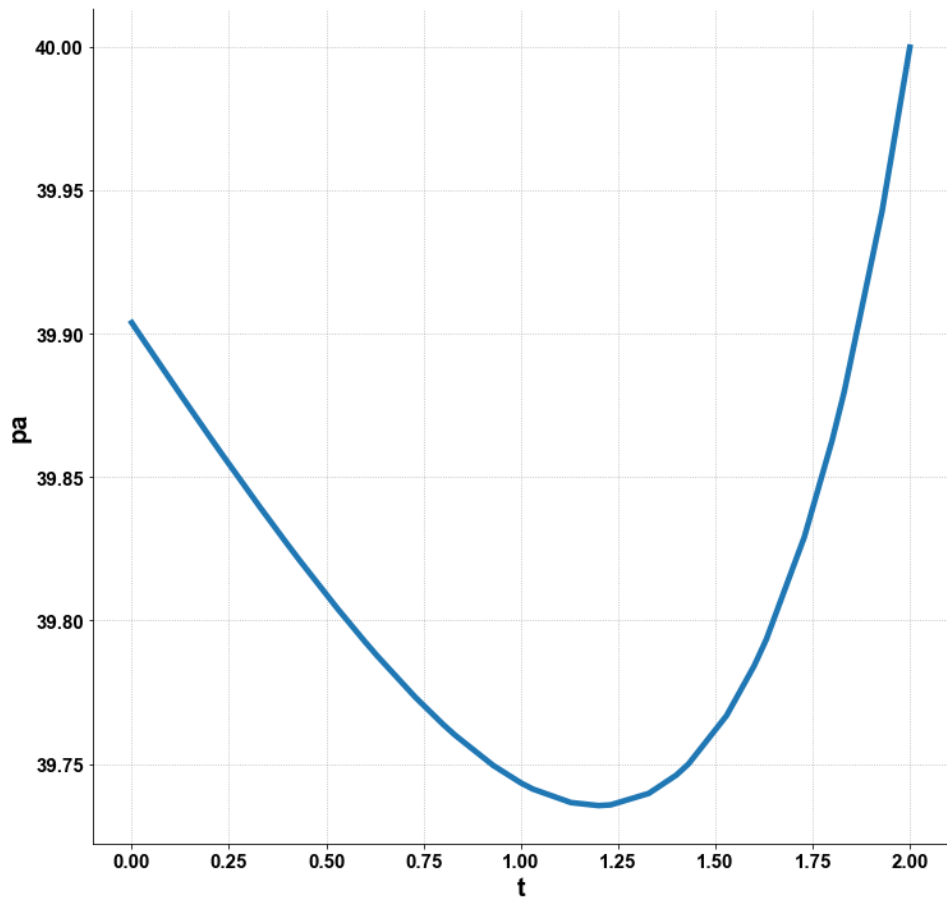


Fig 2a ($\gamma_{AB} = 0$; $\gamma_{BA} = 1$)

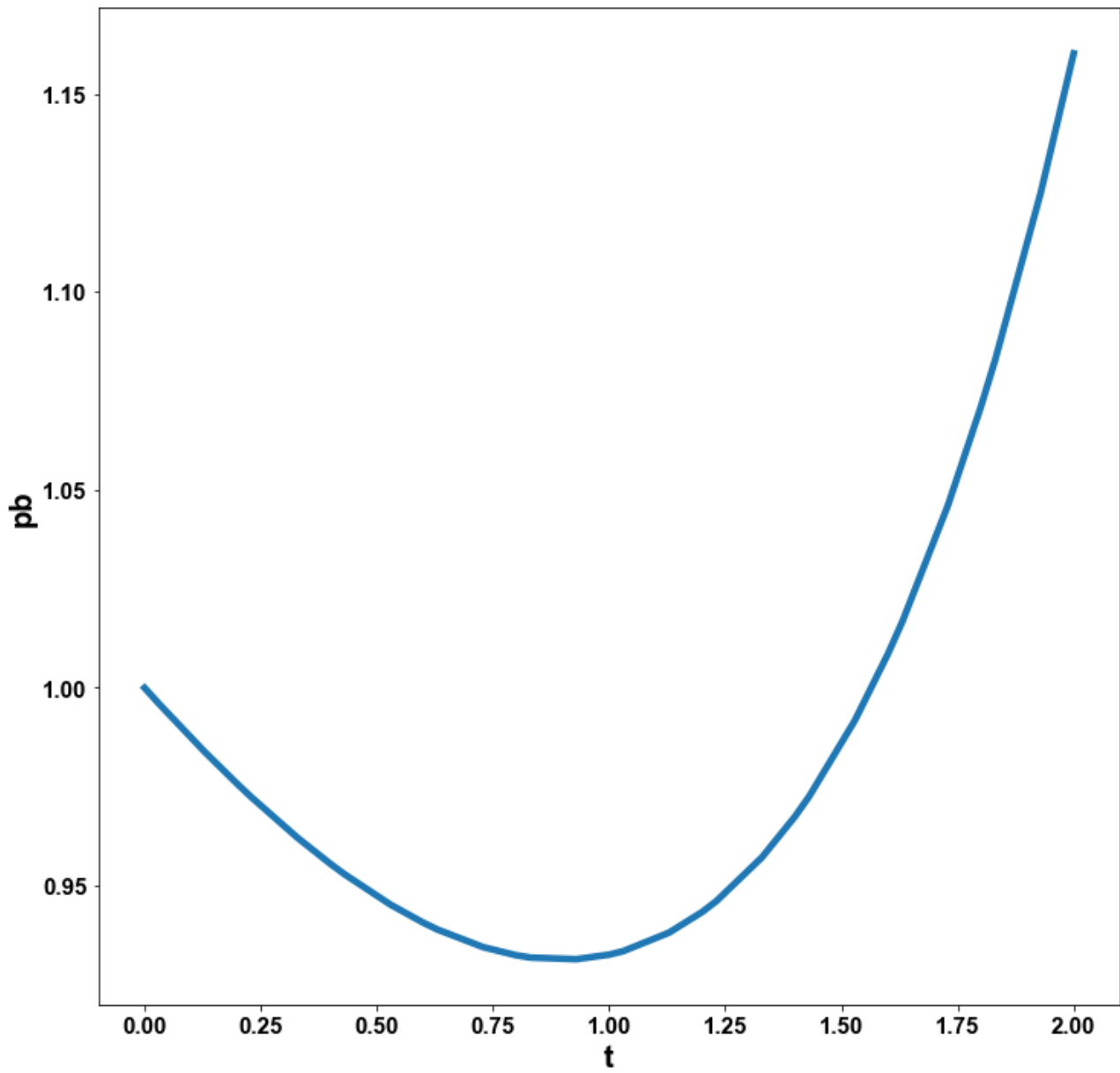


Fig 2b($\gamma_{AB} = 0 ; \gamma_{BA} = 1$)

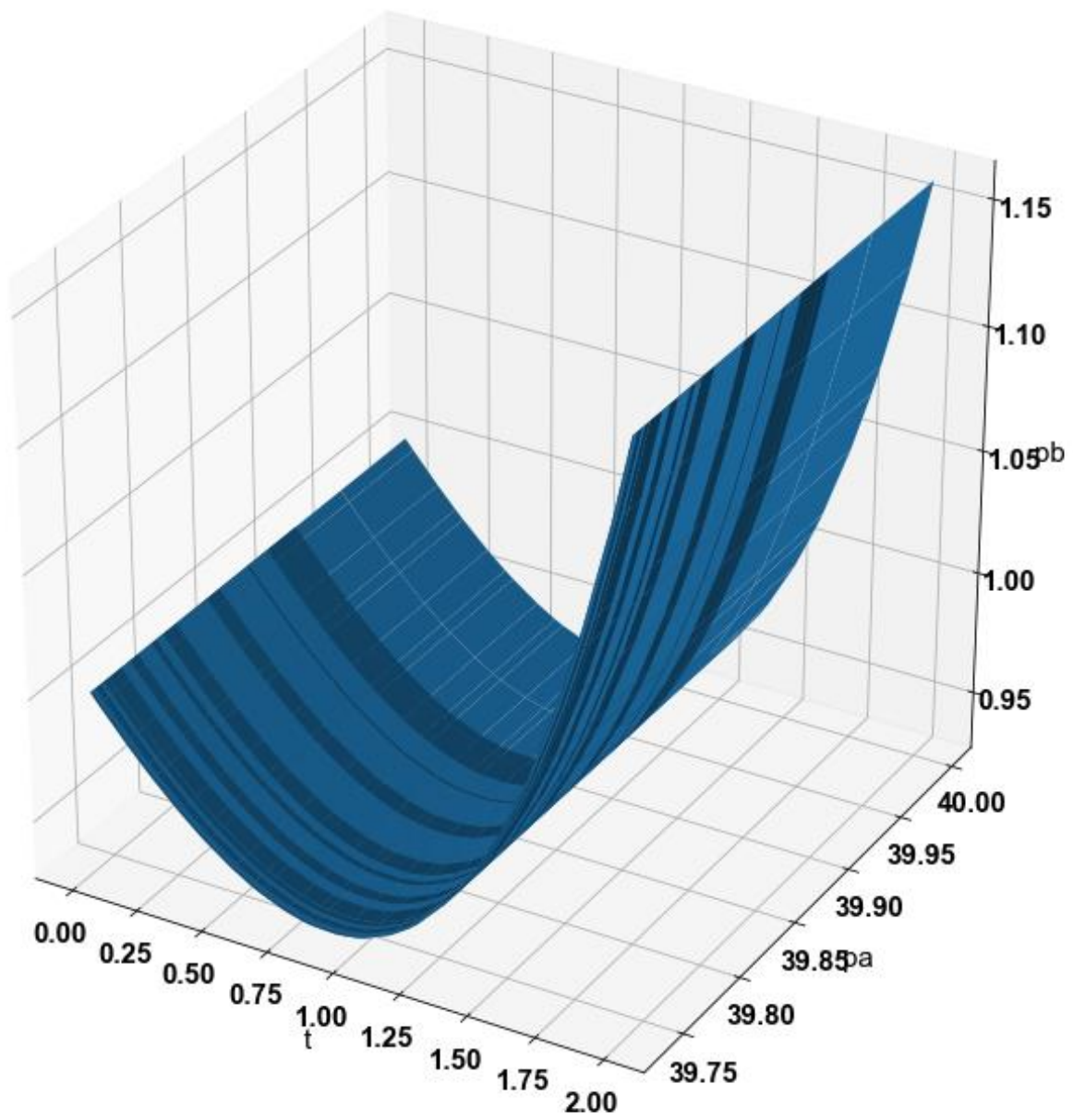


Fig 2c($\gamma_{AB} = 0 ; \gamma_{BA} = 1$)

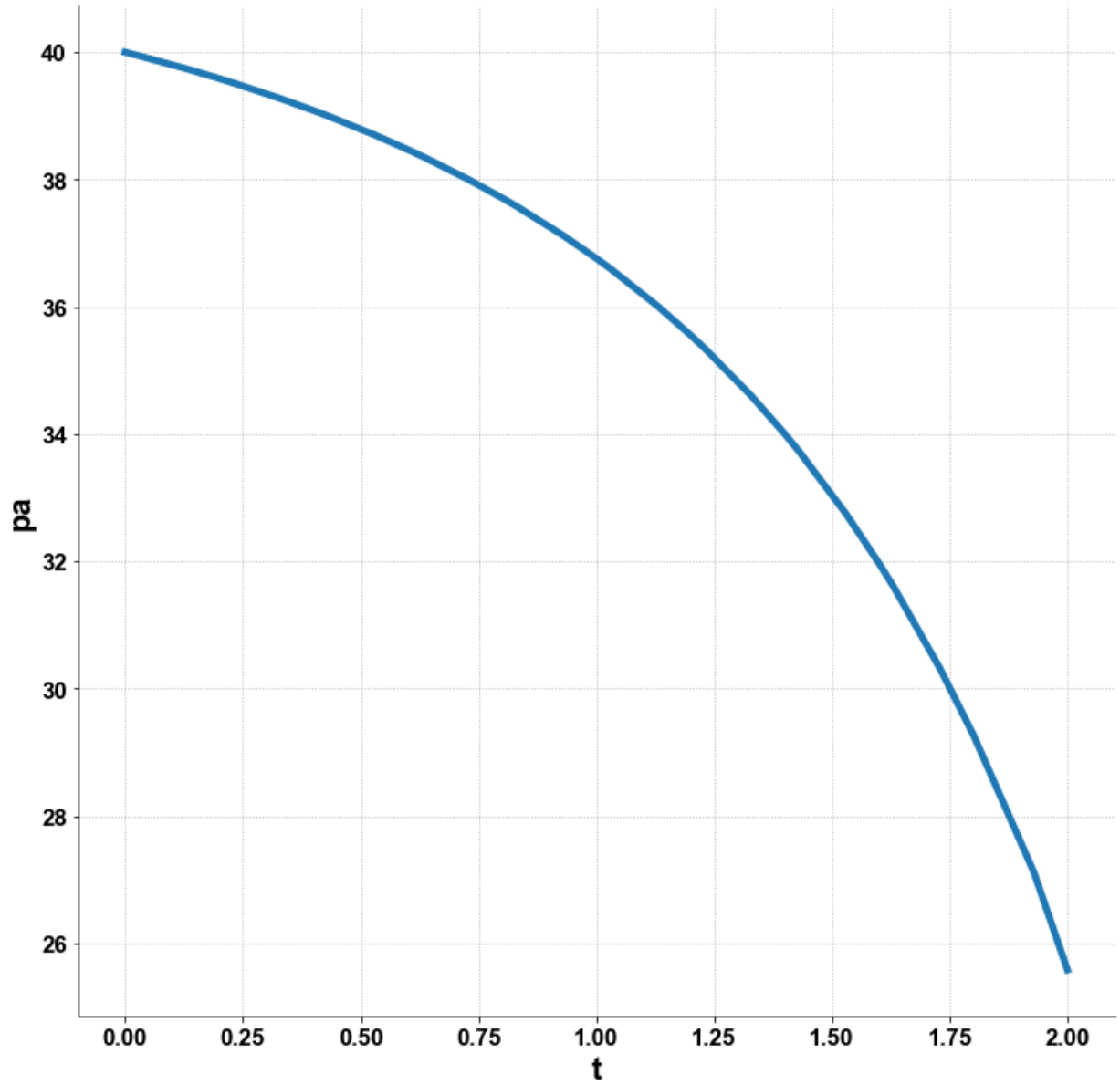


Fig 3a($\gamma_{AB} = 0 ; \gamma_{BA} = -1$)

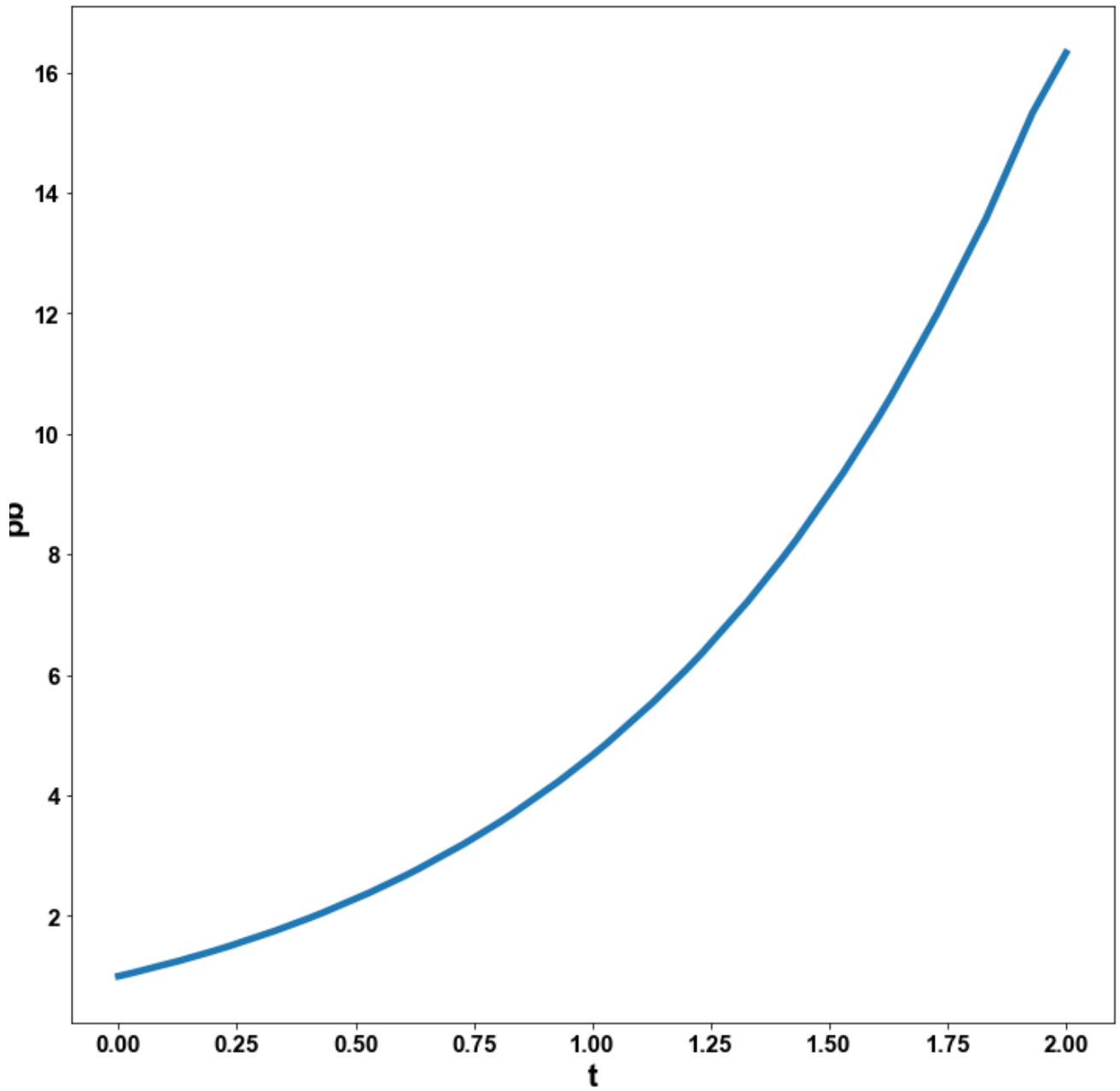


Fig 3b($\gamma_{AB} = 0 ; \gamma_{BA} = -1$)

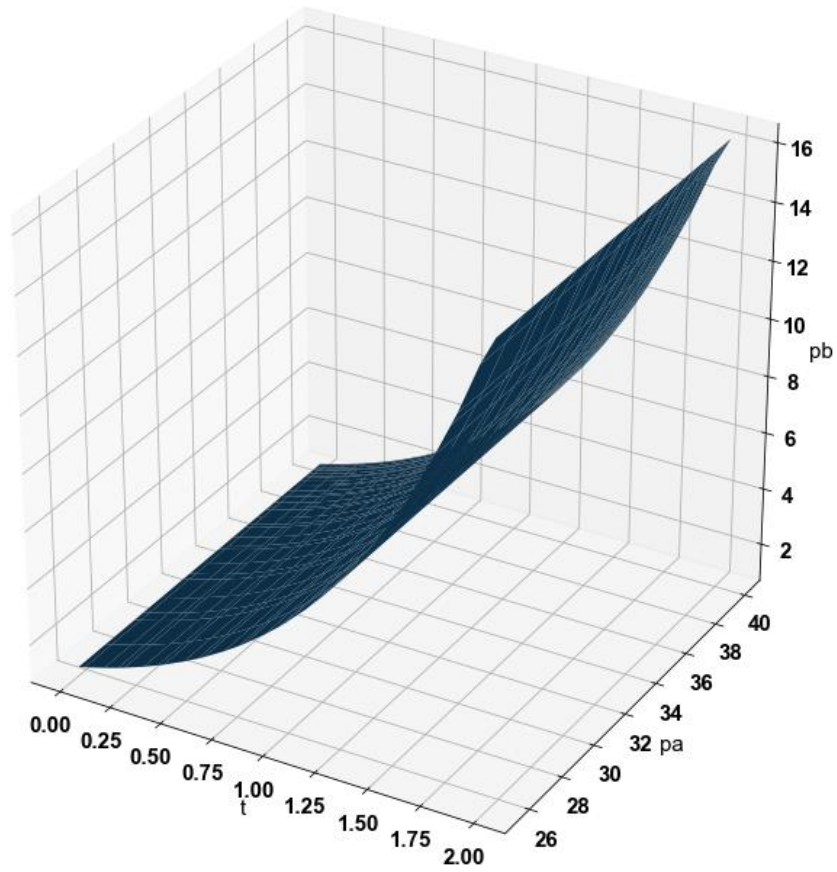


Fig 3c($\gamma_{AB} = 0 ; \gamma_{BA} = -1$)

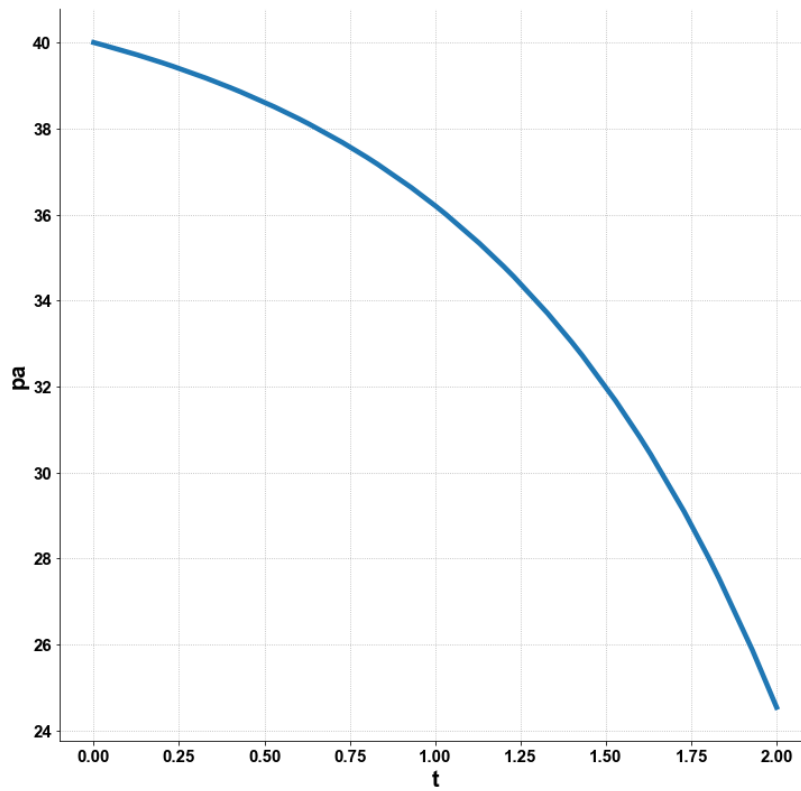


Fig 4a($\gamma_{AB} = 1 ; \gamma_{BA} = 0$)

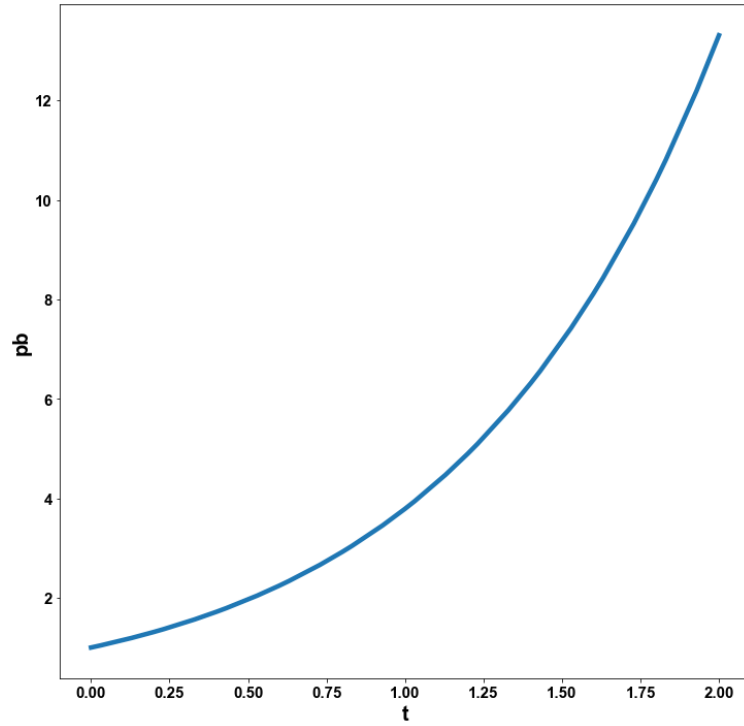


Fig 4b($\gamma_{AB} = 1 ; \gamma_{BA} = 0$)

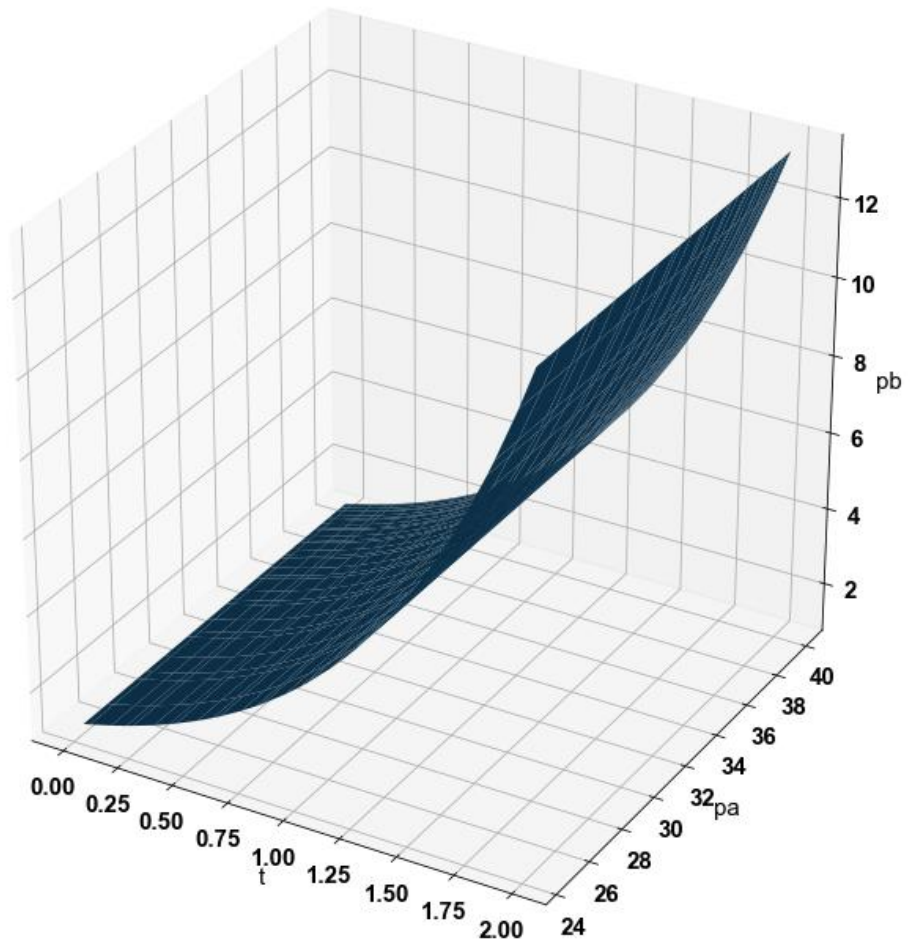


Fig 4c($\gamma_{AB} = 1 ; \gamma_{BA} = 0$)

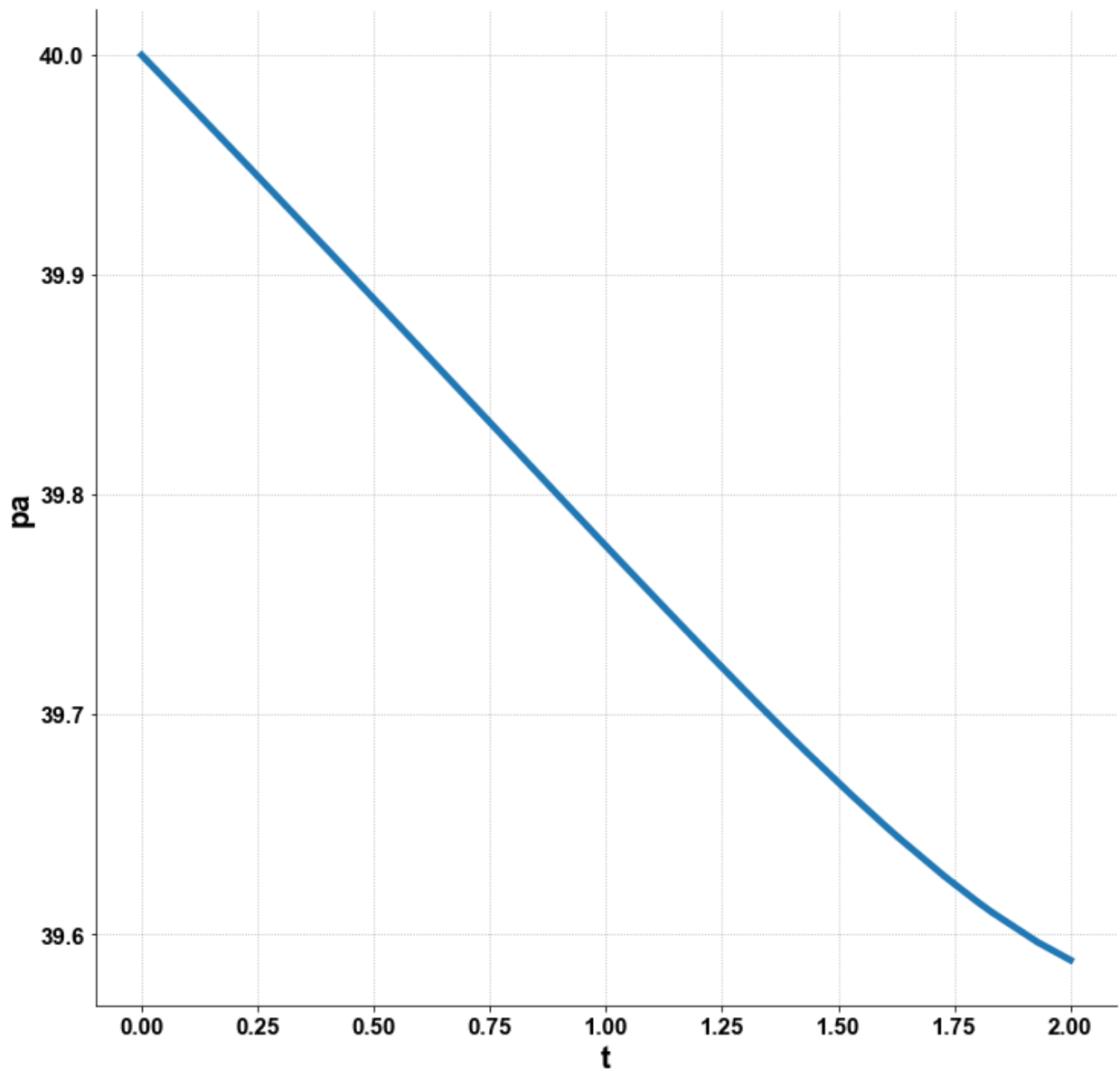


Fig 5a ($\gamma_{AB} = 1 ; \gamma_{BA} = 1$)

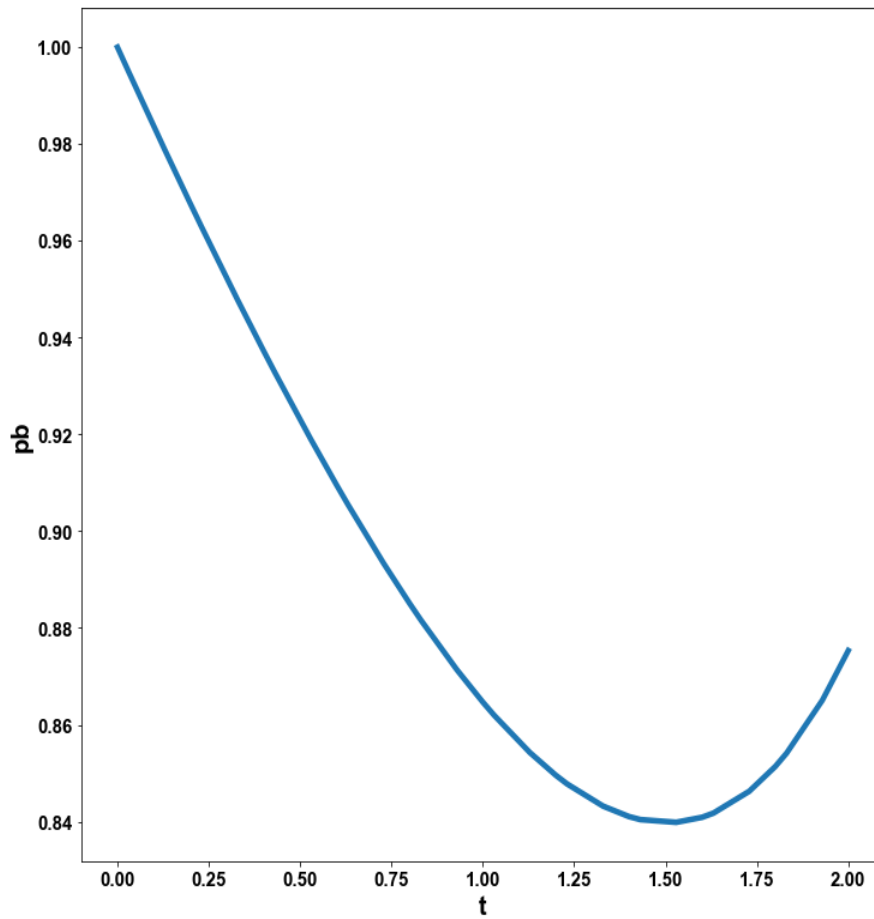


Fig 5b($\gamma_{AB} = 1 ; \gamma_{BA} = 1$)

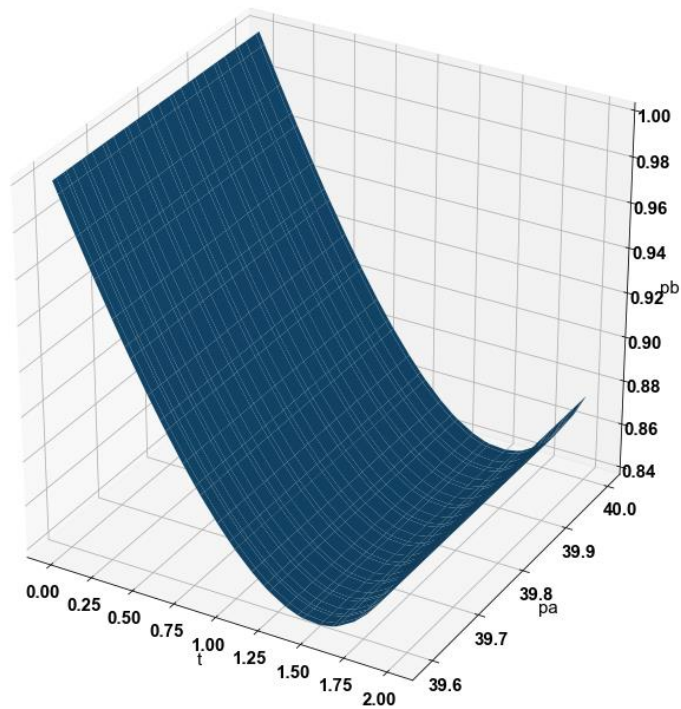


Fig 5c($\gamma_{AB} = 1 ; \gamma_{BA} = 1$)

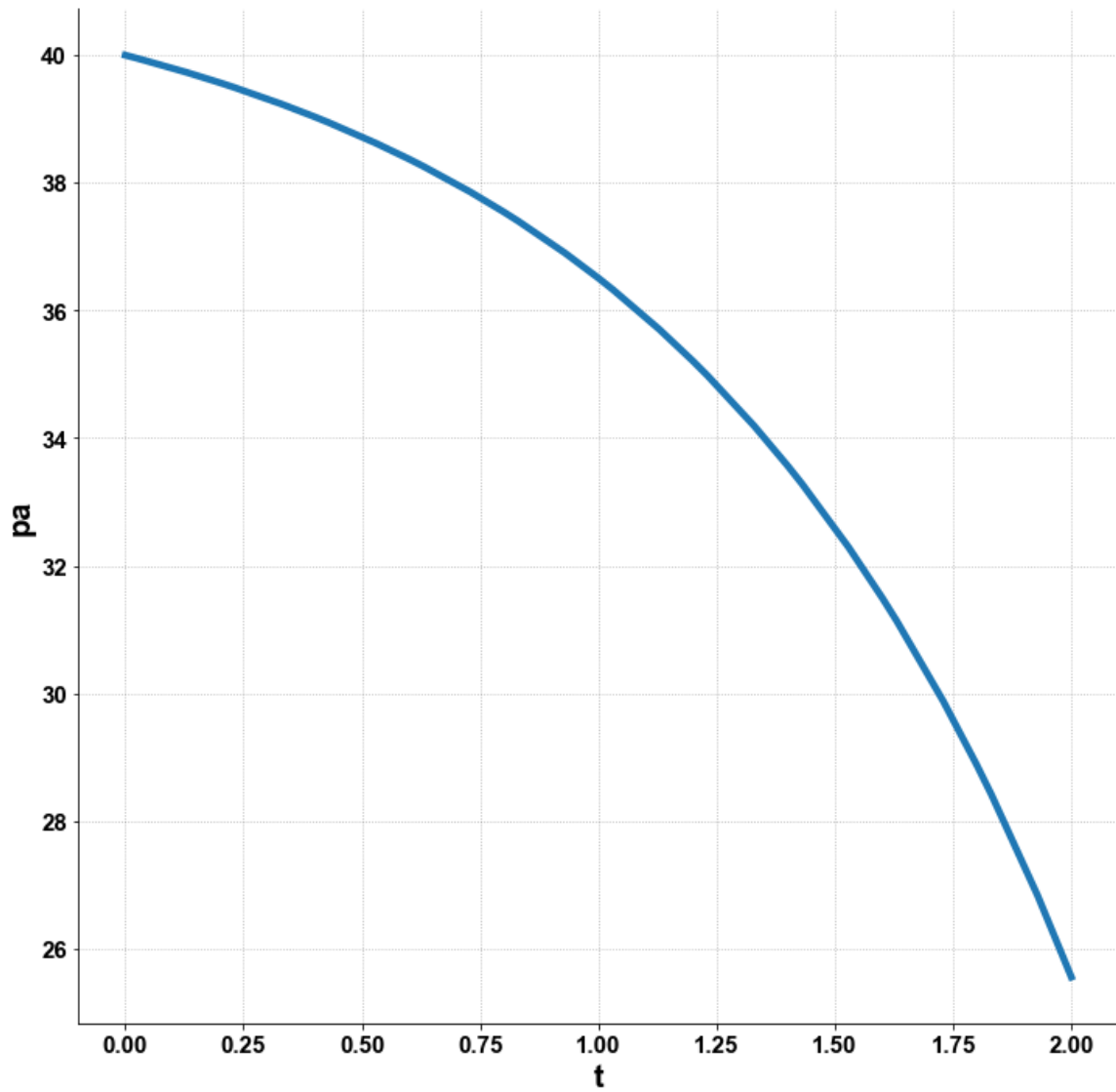


Fig 6a ($\gamma_{AB} = 1 ; \gamma_{BA} = -1$)

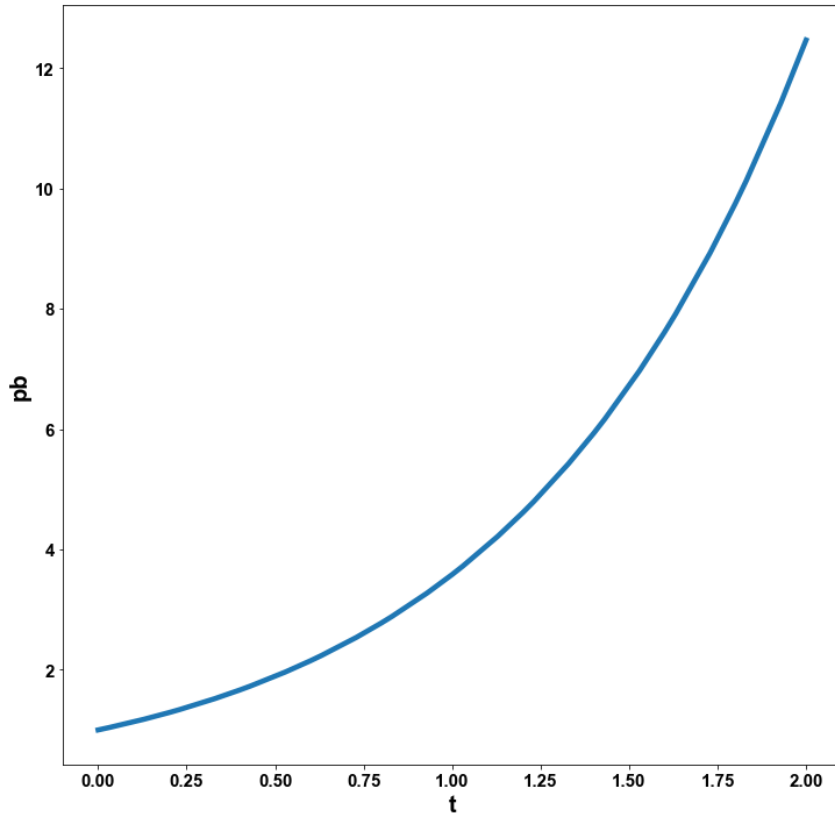


Fig 6b($\gamma_{AB} = 1 ; \gamma_{BA} = -1$)

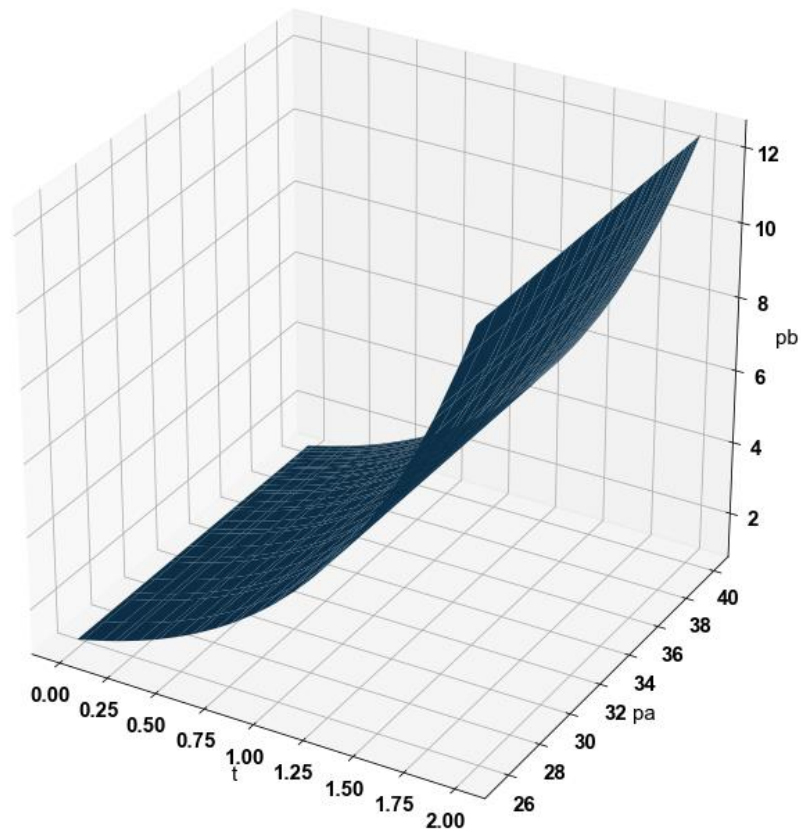


Fig 6c($\gamma_{AB} = 1 ; \gamma_{BA} = -1$)

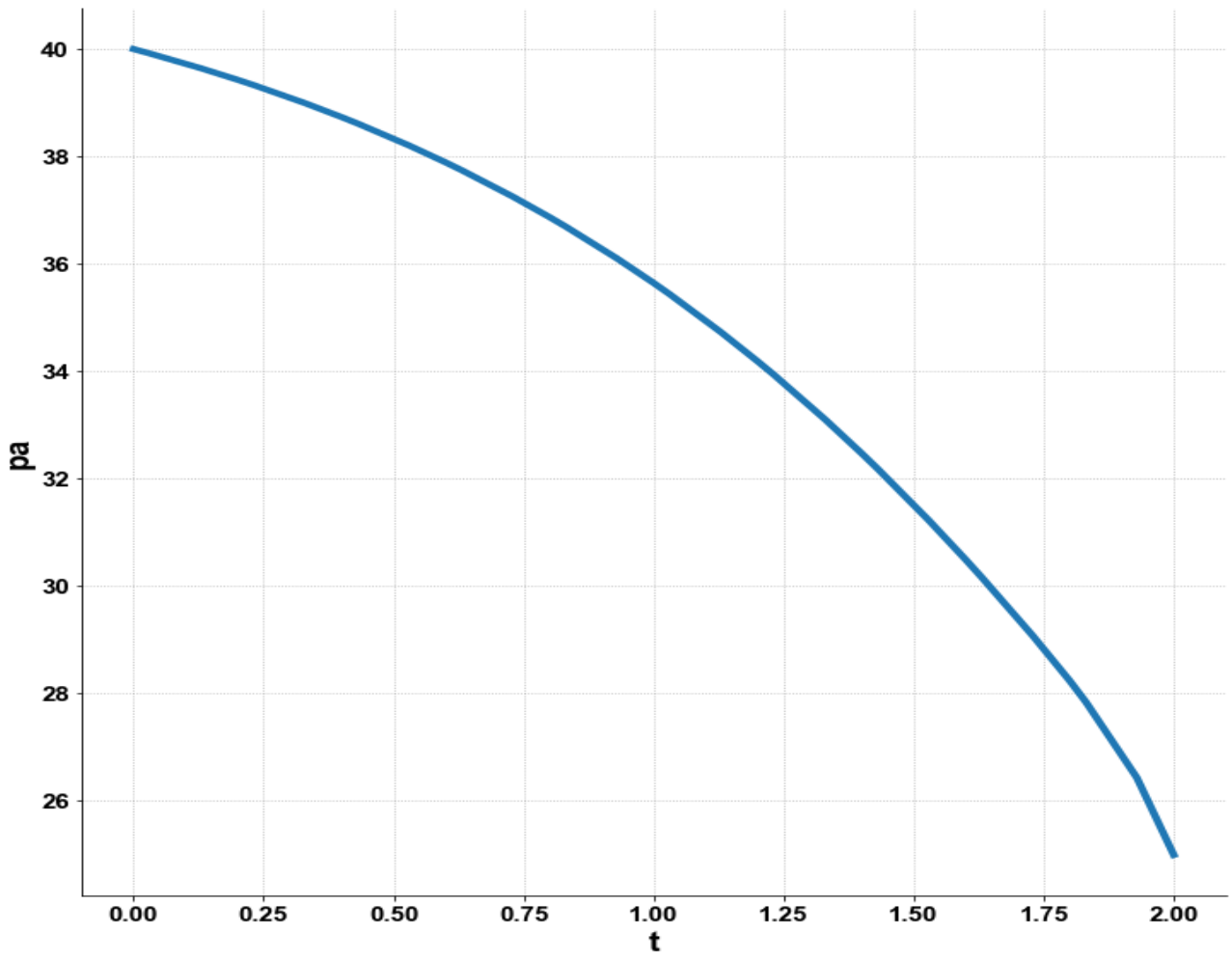


Fig 7a($\gamma_{AB} = -1 ; \gamma_{BA} = 0$)

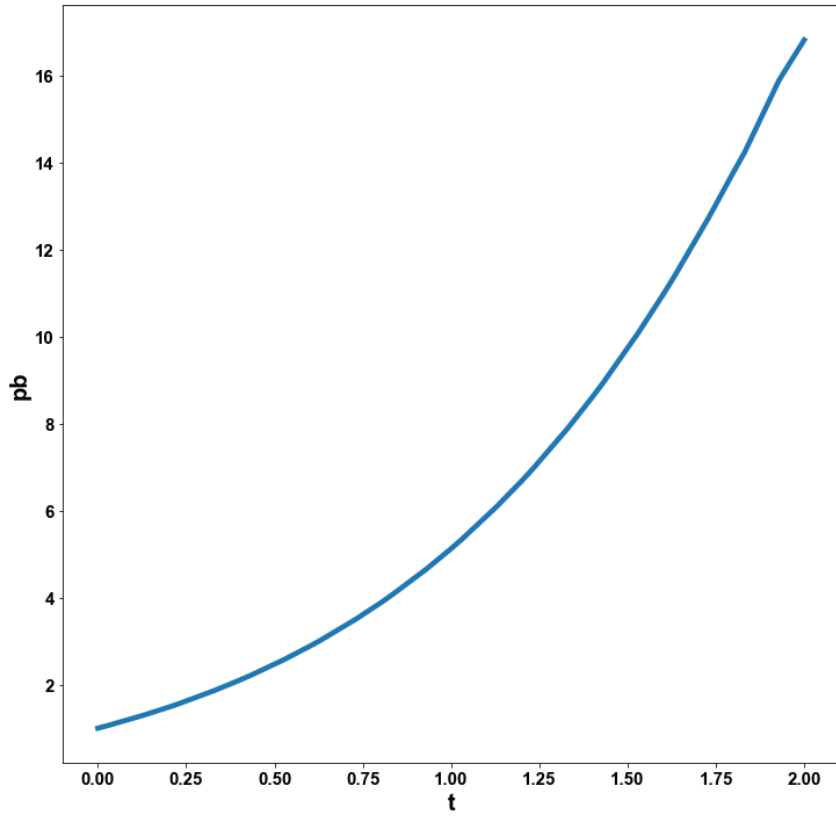


Fig 7b($\gamma_{AB} = -1 ; \gamma_{BA} = 0$)

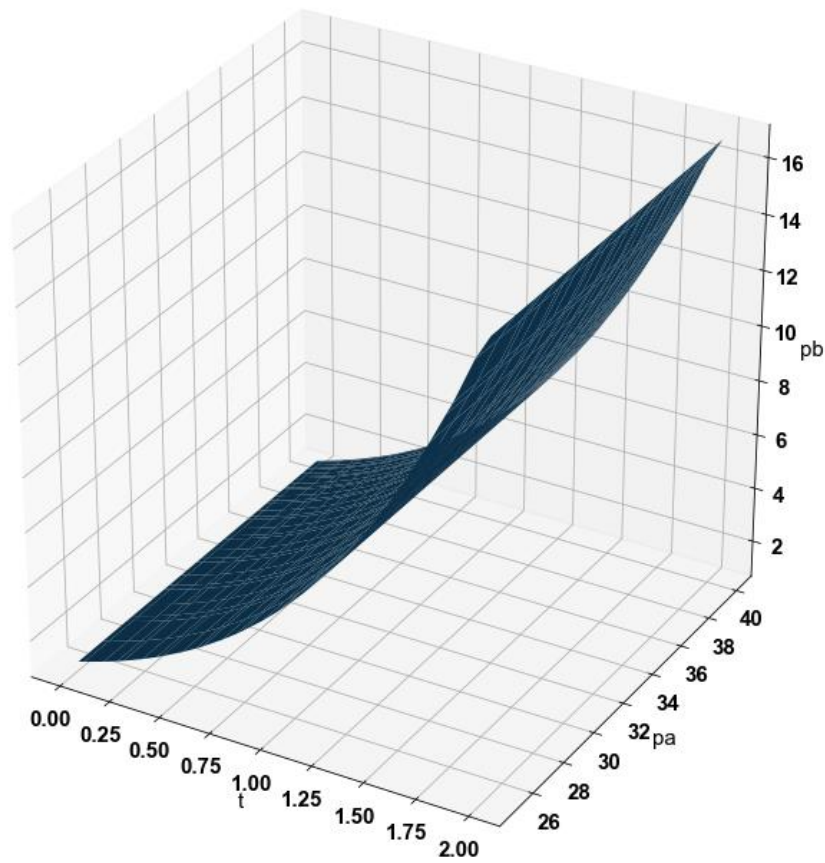


Fig 7c($\gamma_{AB} = -1 ; \gamma_{BA} = 0$)

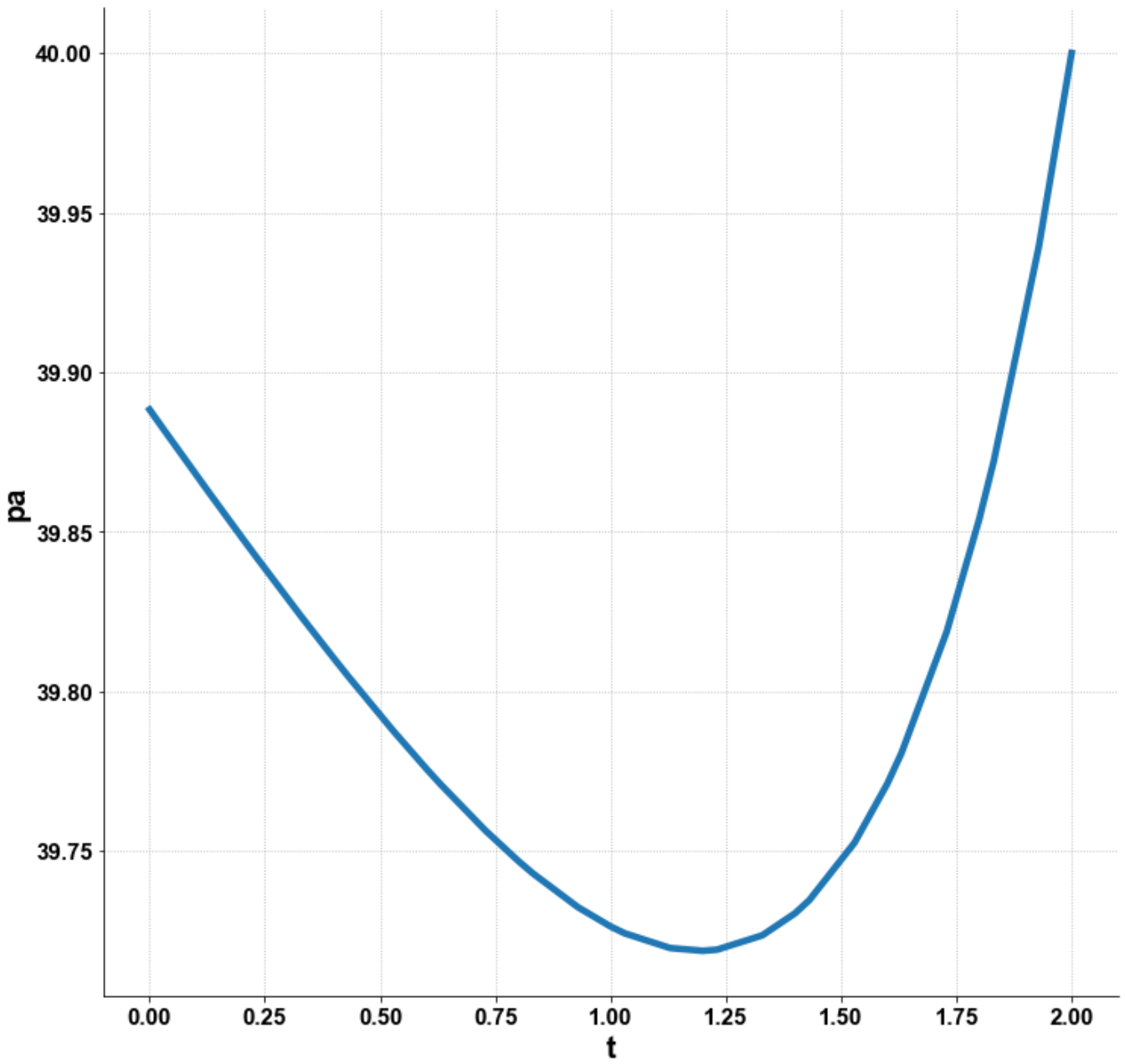


Fig 8a($\gamma_{AB} = -1$; $\gamma_{BA} = 1$)

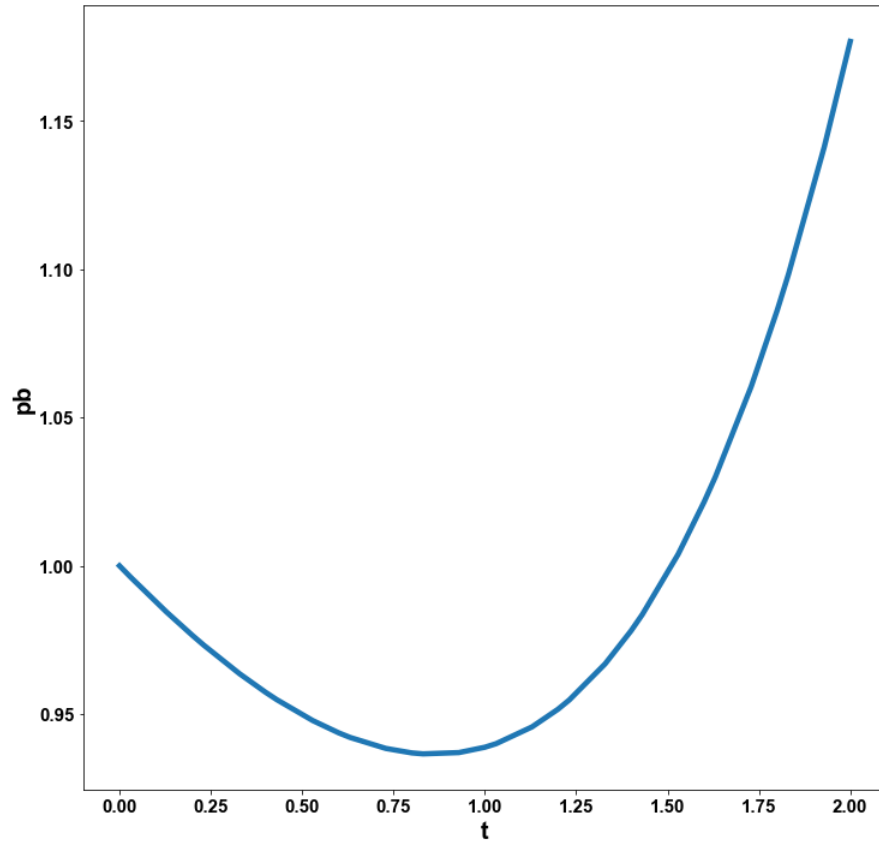


Fig 8b($\gamma_{AB} = -1 ; \gamma_{BA} = 1$)

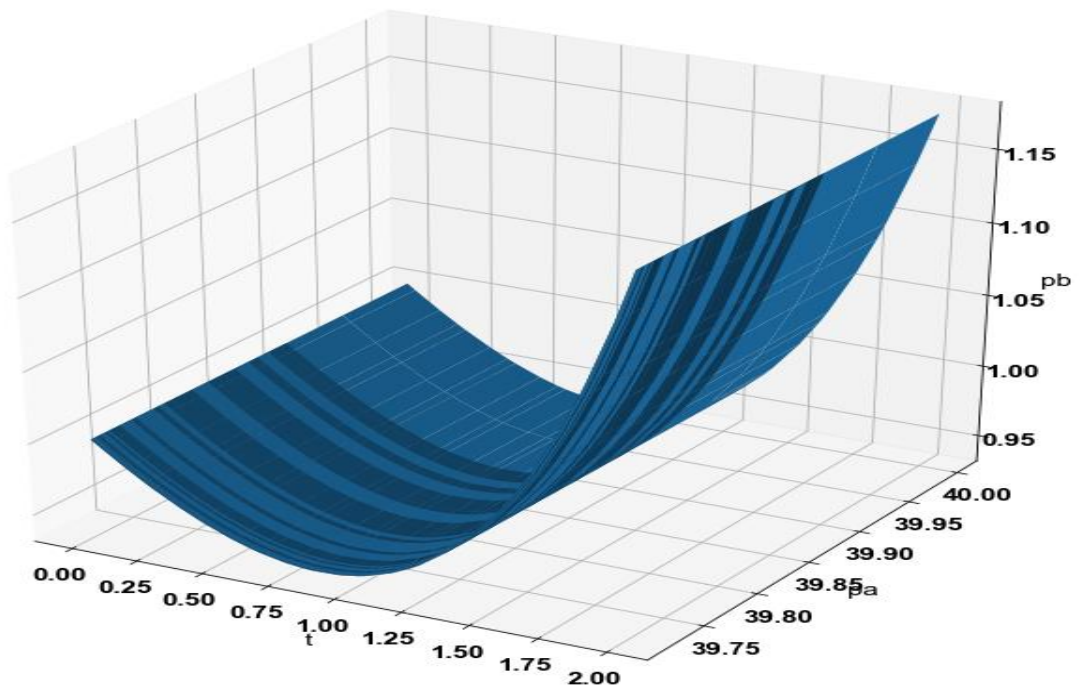


Fig 8c($\gamma_{AB} = -1 ; \gamma_{BA} = 1$)

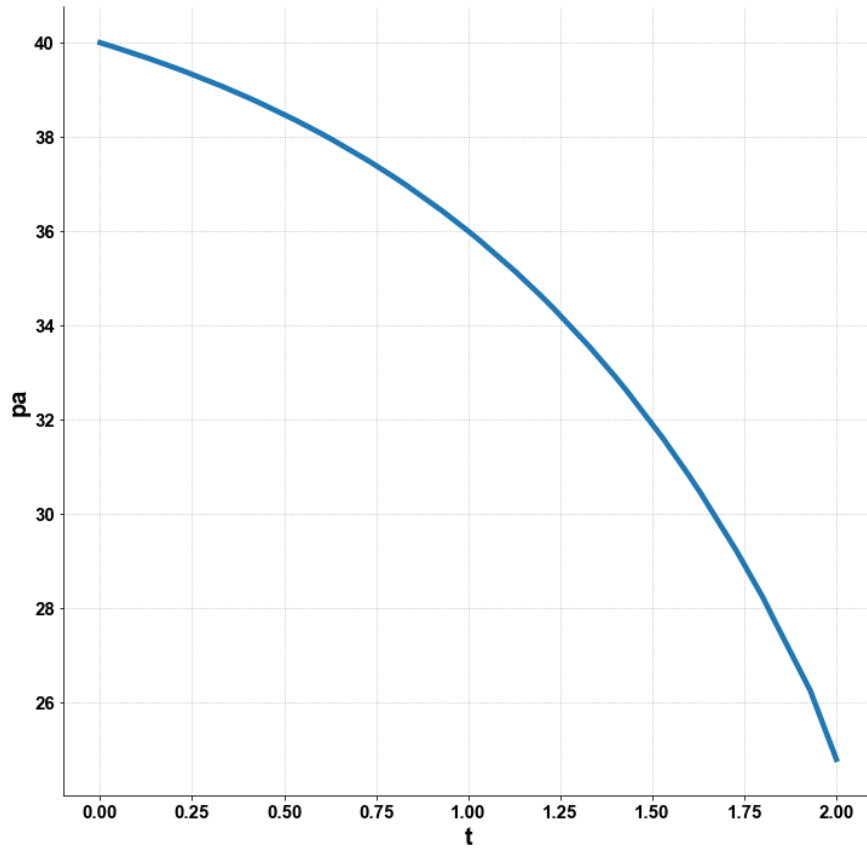


Fig 9a($\gamma_{AB} = -1$; $\gamma_{BA} = -1$)

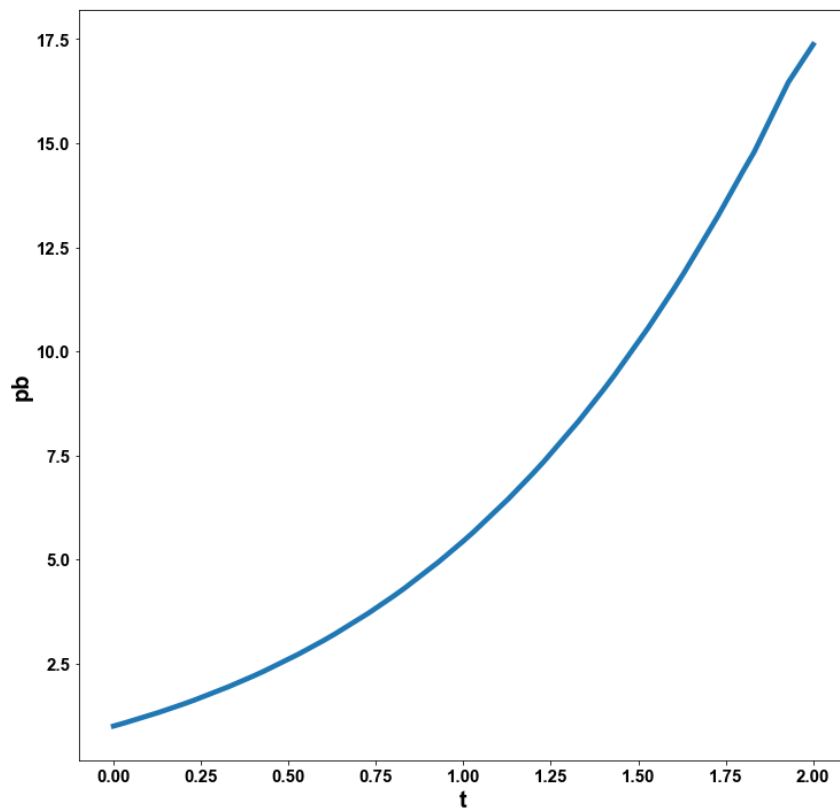


Fig 9b($\gamma_{AB} = -1$; $\gamma_{BA} = -1$)

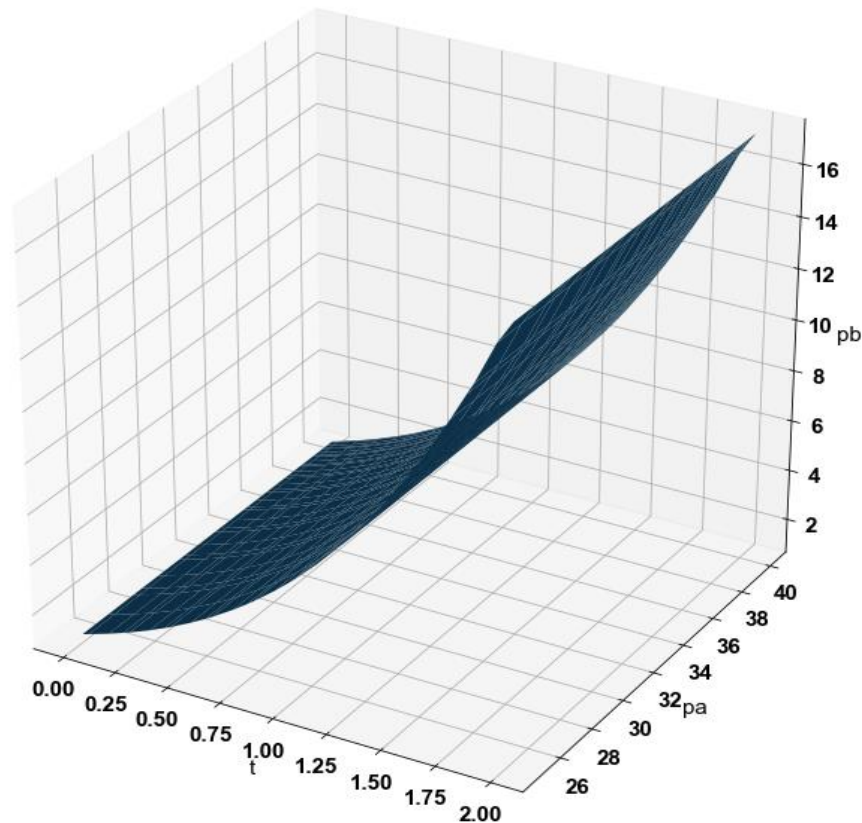


Fig 9c($\gamma_{AB} = -1$; $\gamma_{BA} = -1$)

5. Conclusions and Future Work

Multiobjective nonlinear model predictive control of the dynamics in the microbial consortium involving two active organisms was performed. The dynamics involve competition, amensalism, parasitism, neutralism, commensalism and cooperation. It is shown that when the species that produces the required product is favorable to the other species there is an initial decrease in the required product before an increase takes place. A waiting period is necessary before the concentration of the required product starts to increase. Future work will involve more than two active organisms in the microbiome.

Data Availability Statement

The authors confirm that the data supporting the findings of this study are available within the article.

References

1. Fredrickson, A. G., & Stephanopoulos, G. (1981). Microbial competition. *Science*, 213(4511), 972-979.
2. Du, P., Zhao, H., Zhang, H., Wang, R., Huang, J., Tian, Y., ... & Lou, C. (2020). De novo design of an intercellular signaling toolbox for multi-channel cell-cell communication and biological computation. *Nature communications*, 11(1), 4226.
3. Brenner, K., You, L., & Arnold, F. H. (2008). Engineering microbial consortia: a new frontier in synthetic biology. *Trends in biotechnology*, 26(9), 483-489.
4. Tsoi, R., Dai, Z., & You, L. (2019). Emerging strategies for engineering microbial communities. *Biotechnology advances*, 37(6), 107372.
5. McCarty, N. S., & Ledesma-Amaro, R. (2019). Synthetic biology tools to engineer microbial communities for biotechnology. *Trends in biotechnology*, 37(2), 181-197.
6. Jawed, K., Yazdani, S. S., & Koffas, M. A. (2019). Advances in the development and application of microbial consortia for metabolic engineering. *Metabolic engineering communications*, 9, e00095.
7. Minty, J. J., Singer, M. E., Scholz, S. A., Bae, C. H., Ahn, J. H., Foster, C. E., ... & Lin, X. N. (2013). Design and characterization of synthetic fungal-bacterial consortia for direct production of isobutanol from cellulosic biomass. *Proceedings of the National Academy of Sciences*, 110(36), 14592-14597.
8. Arora, D., Gupta, P., Jaglan, S., Roullier, C., Grovel, O., & Bertrand, S. (2020). Expanding the chemical diversity through microorganisms co-culture: Current status and outlook. *Biotechnology Advances*, 40, 107521.
9. Wang, R., Zhao, S., Wang, Z., & Koffas, M. A. (2020). Recent advances in modular co-culture engineering for synthesis of natural products. *Current Opinion in Biotechnology*, 62, 65-71.
10. Xu, P. (2021). Dynamics of microbial competition, commensalism, and cooperation and its implications for coculture and microbiome engineering. *Biotechnology and bioengineering*, 118(1), 199-209.
11. Zhang, H., & Wang, X. (2016). Modular co-culture engineering, a new approach for metabolic engineering. *Metabolic engineering*, 37, 114-121.

12. Stephens, K., Pozo, M., Tsao, C. Y., Hauk, P., & Bentley, W. E. (2019). Bacterial co-culture with cell signaling translator and growth controller modules for autonomously regulated culture composition. *Nature communications*, 10(1), 4129.
13. Marsafari, M., Ma, J., Koffas, M., & Xu, P. (2020). Genetically-encoded biosensors for analyzing and controlling cellular process in yeast. *Current Opinion in Biotechnology*, 64, 175-182.
14. Rugbjerg, P., Sarup-Lytzen, K., Nagy, M., & Sommer, M. O. A. (2018). Synthetic addiction extends the productive life time of engineered *Escherichia coli* populations. *Proceedings of the National Academy of Sciences*, 115(10), 2347-2352.
15. Lv, Y., Gu, Y., Xu, J., Zhou, J., & Xu, P. (2020). Coupling metabolic addiction with negative autoregulation to improve strain stability and pathway yield. *Metabolic Engineering*, 61, 79-88.
16. Lv, Y., Qian, S., Du, G., Chen, J., Zhou, J., & Xu, P. (2019). Coupling feedback genetic circuits with growth phenotype for dynamic population control and intelligent bioproduction. *Metabolic engineering*, 54, 109-116.
17. Said, S. B., Tecon, R., Borer, B., & Or, D. (2020). The engineering of spatially linked microbial consortia—potential and perspectives. *Current opinion in biotechnology*, 62, 137-145.
18. Dai, Z., Lee, A. J., Roberts, S., Sysoeva, T. A., Huang, S., Dzuricky, M., ... & You, L. (2019). Versatile biomanufacturing through stimulus-responsive cell–material feedback. *Nature Chemical Biology*, 15(10), 1017-1024.
19. Davies, J., & Davies, D. (2010). Origins and evolution of antibiotic resistance. *Microbiology and molecular biology reviews*, 74(3), 417-433.
20. Song, H. S., Cannon, W. R., Beliaev, A. S., & Konopka, A. (2014). Mathematical modeling of microbial community dynamics: a methodological review. *Processes*, 2(4), 711-752.
21. Kong, W., Meldgin, D. R., Collins, J. J., & Lu, T. (2018). Designing microbial consortia with defined social interactions. *Nature Chemical Biology*, 14(8), 821-829.
22. Succurro, A., & Ebenhöf, O. (2018). Review and perspective on mathematical modeling of microbial ecosystems. *Biochemical Society Transactions*, 46(2), 403-412.
23. Han, K., & Levenspiel, O. (1988). Extended Monod kinetics for substrate, product, and cell inhibition. *Biotechnology and bioengineering*, 32(4), 430-447.
24. Levenspiel, O. (1980). The Monod equation: a revisit and a generalization to product inhibition situations. *Biotechnology and bioengineering*, 22(8), 1671-1687.
25. Luong, J. H. T. (1987). Generalization of Monod kinetics for analysis of growth data with substrate inhibition. *Biotechnology and Bioengineering*, 29(2), 242-248.
26. Monod, J. (1949). The growth of bacterial cultures. *Annual review of microbiology*, 3(1), 371-394.
27. Tsuchiya, H. M., Drake, J. F., Jost, J. L., & Fredrickson, A. G. (1972). Predator-prey interactions of *Dictyostelium discoideum* and *Escherichia coli* in continuous culture. *Journal of Bacteriology*, 110(3), 1147-1153.
28. Lotka, A. J. (1926). *Science Progress in the Twentieth Century* (1919-1933), *Elements of physical biology* (Vol. 21, pp. 341–343).
29. Volterra, V. (1926). Fluctuations in the abundance of a species considered mathematically. *Nature*, 118(2972), 558-560.
30. Schwabe, R. F., & Jobin, C. (2013). The microbiome and cancer. *Nature Reviews Cancer*, 13(11), 800-812.
31. Youngster, I., Sauk, J., Pindar, C., Wilson, R. G., Kaplan, J. L., Smith, M. B., ... & Hohmann, E. L. (2014). Fecal microbiota transplant for relapsing *Clostridium difficile* infection using a frozen inoculum from unrelated donors: a randomized, open-label, controlled pilot study. *Clinical infectious diseases*, 58(11), 1515-1522.
32. Stefka, A. T., Feehley, T., Tripathi, P., Qiu, J., McCoy, K., Mazmanian, S. K., ... & Nagler, C. R. (2014). Commensal bacteria protect against food allergen sensitization. *Proceedings of the National Academy of Sciences*, 111(36), 13145-13150.
33. Kostic, A. D., Gevers, D., Siljander, H., Vatanen, T., Hyötyläinen, T., Hämäläinen, A. M., ... & DIABIMMUNE Study Group. (2015). The dynamics of the human infant gut microbiome in development and in progression toward type 1 diabetes. *Cell host & microbe*, 17(2), 260-273.
34. Wlodarska, M., Kostic, A. D., & Xavier, R. J. (2015). An integrative view of microbiome-host interactions in inflammatory bowel diseases. *Cell host & microbe*, 17(5), 577-591.
35. Hall, A. B., Tolonen, A. C., & Xavier, R. J. (2017). Human genetic variation and the gut microbiome in disease. *Nature Reviews Genetics*, 18(11), 690-699.
36. Stein, R. R., Bucci, V., Toussaint, N. C., Buffie, C. G., Räscher, G., Pamer, E. G., ... & Xavier, J. B. (2013). Ecological modeling from time-series inference: insight into dynamics and stability of intestinal microbiota. *PLoS computational biology*, 9(12), e1003388.
37. de Vos, M. G., Zagorski, M., McNally, A., & Bollenbach, T. (2017). Interaction networks, ecological stability, and collective antibiotic tolerance in polymicrobial infections. *Proceedings of the National Academy of Sciences*, 114(40), 10666-10671.
38. Hassani, M. A., Durán, P., & Hacquard, S. (2018). Microbial interactions within the plant holobiont. *Microbiome*, 6, 1-17.
39. Larimer, A. L., Clay, K., & Bever, J. D. (2014). Synergism and context dependency of interactions between arbuscular mycorrhizal fungi and rhizobia with a prairie legume. *Ecology*, 95(4), 1045-1054.
40. Lima-Mendez, G., Faust, K., Henry, N., Decelle, J., Colin, S., Carcillo, F., ... & Raes, J. (2015). Determinants of community structure in the global plankton interactome. *Science*, 348(6237), 1262073.
41. Faust, K., & Raes, J. (2012). Microbial interactions: from networks to models. *Nature Reviews Microbiology*, 10(8), 538-550.
42. Widder, S., Allen, R. J., Pfeiffer, T., Curtis, T. P., Wiuf, C., Sloan, W. T., ... & Soyer, O. S. (2016). Challenges in microbial ecology: building predictive understanding of community function and dynamics. *The ISME journal*, 10(11),

43. Coyte, K. Z., Schluter, J., & Foster, K. R. (2015). The ecology of the microbiome: networks, competition, and stability. *Science*, 350(6261), 663-666.
44. Gonze, D., Lahti, L., Raes, J., & Faust, K. (2017). Multi-stability and the origin of microbial community types. *The ISME journal*, 11(10), 2159-2166.
45. Faith, J. J., McNulty, N. P., Rey, F. E., & Gordon, J. I. (2011). Predicting a human gut microbiota's response to diet in gnotobiotic mice. *Science*, 333(6038), 101-104.
46. Flores-Tlacuahuac, A., Morales, P., & Rivera-Toledo, M. (2012). Multiobjective nonlinear model predictive control of a class of chemical reactors. *Industrial & Engineering Chemistry Research*, 51(17), 5891-5899.
47. Sridhar, L. N. (2022). Multiobjective optimization and non-linear model predictive control of the continuous fermentation process involving *Saccharomyces Cerevisiae*. *Biofuels*, 13(2), 249-264.
48. Miettinen, K. (1999). *Nonlinear multiobjective optimization* (Vol. 12). Springer Science & Business Media.z
49. Hart, W. E., Laird, C. D., Watson, J. P., Woodruff, D. L., Hackebeil, G. A., Nicholson, B. L., & Siirola, J. D. (2017). *Pyomo-optimization modeling in python* (Vol. 67, p. 277). Berlin: Springer.
50. Tawarmalani, M., & Sahinidis, N. V. (2005). A polyhedral branch-and-cut approach to global optimization. *Mathematical programming*, 103(2), 225-249.
51. Bussieck, M. R., & Meeraus, A. (2004). *General algebraic modeling system (GAMS). Modeling languages in mathematical optimization*, 137-157.

Copyright: ©2023 Lakshmi N Sridhar. This is an open-access article distributed under the terms of the Creative Commons Attribution License, which permits unrestricted use, distribution, and reproduction in any medium, provided the original author and source are credited.